SCOPING ANALYSIS OF HYDROGEN ACCUMULATION AND MIGRATION UNDER REDUCING REPOSITORY CONDITIONS

Prepared for

U.S. Nuclear Regulatory Commission
Contract NRC–HQ–12–C–02–0089

Prepared by

Pavan K. Shukla[1]
Tae Ahn[2]
Xihua He[1]

[1]Center for Nuclear Waste Regulatory Analyses
San Antonio, Texas

[2]U.S. Nuclear Regulatory Commission
Washington, DC

May 2017

CONTENTS

FIGURES

TABLES

ACKNOWLEDGMENTS

This report was prepared to document work performed by the Center for Nuclear Waste Regulatory Analyses (CNWRA®) for the U.S. Nuclear Regulatory Commission (NRC) under Contract No. NRC–HQ–12–C–02–0089. The activities reported were performed on behalf of the NRC Office of Nuclear Material Safety and Safeguards, Division of Spent Fuel Management. The report is an independent product of CNWRA and does not necessarily reflect the views or regulatory position of NRC. The NRC staff views expressed herein are preliminary and do not constitute a final judgment or determination of the matters addressed or of the acceptability of any licensing action that may be under consideration at NRC. The authors thank Osvaldo Pensado for technical review and David Pickett for editorial and programmatic reviews. J. Gwo, R. Fedors, and T. Cao (NRC) also provided constructive comments. The authors also appreciate Arturo Ramos for providing word processing support in preparation of this document.

QUALITY OF DATA, ANALYSES, AND CODE DEVELOPMENT DATA

DATA, ANALYSES AND CODES: All CNWRA-generated data contained in this report meet quality assurance requirements described in the Center for Nuclear Waste Regulatory Analyses Quality Assurance Manual. Sources of other data should be consulted for determining the level of quality of those data. The work presented in this report is documented in Scientific Notebook 1250 (Poerner and Shukla, 2015).

The commercial computer software MATLAB® (Mathworks®, 2008) Version R2013b was used in the analyses contained in this report.

REFERENCES:

Mathworks. "MATLAB User's Guide." Natick, Massachusetts: The MathWorks, Inc. 2008.

Poerner, M. and P. Shukla. "Conduct Electrochemical and Other Experiments to Determine Dissolution of SIMFUEL Under Various Conditions." Scientific Notebook 1250. San Antonio, Texas: Center for Nuclear Waste Regulatory Analyses. pp. 94–107. 2015.

EXECUTIVE SUMMARY

Hydrogen may be generated by anoxic corrosion of metallic components and by radiolysis of water in a deep geologic repository for radioactive waste. Hydrogen is expected to start forming and accumulating as soon as groundwater contacts the high-level waste container. The dissolved hydrogen is expected to provide a beneficial effect on dissolution of spent nuclear fuel under reducing conditions.

This report presents a simplified computation of the hydrogen concentration in buffer material porewater in a hypothetical deep repository. A model was developed to determine when the hydrogen concentration will reach saturation, assuming all hydrogen is formed in solution. The model was exercised to estimate the dissolved hydrogen concentration in the porewater as a direct function of carbon steel and copper corrosion rates, repository depth, and properties of a buffer composed of different materials (clay and sand-based).

The computations indicate that for low corrosion rates of carbon steel in the clay buffer, the hydrogen concentration in the porewater directly in contact with the waste package may saturate in approximately 800 years (minimal time ignoring degassing). The dissolved hydrogen concentration increases with time and, for a given time, the concentration increases with increasing depth with respect to the water table. The model results also indicate that for high corrosion rates of carbon steel in the clay buffer, the hydrogen concentration in the porewater directly in contact with the waste package could saturate within a few days. For this case, the dissolved hydrogen concentration also increases with time and increasing depth. The overall shape of the hydrogen concentration versus time curve at the waste package and buffer interface did not change for the two cases. The model results for copper behave similarly to the carbon steel results, although the rates of hydrogen generation and accumulation are slower. For low copper corrosion rates, the dissolved hydrogen concentration would reach saturation in approximately 50 million years or more. For high copper corrosion rates, the saturation could be reached in approximately 50 years.

In this project, the minimum time to hydrogen saturation is used as a metric to examine a range of possibilities. The corrosion rate is an important parameter, along with buffer properties, in determining the accumulation and migration of hydrogen. Most analyses in the literature, as well as the scoping calculations in this report, implement simplified assumptions to optimize gas buildup effects. The analyses in general ignore couplings that would tend to reduce gas accumulation, such as local decreases in water activity due to the gas buildup and associated reduction in corrosion rates and hydrogen generation. Developing fully coupled models allowing detailed examination of the relevance of gas accumulation is challenging. Caution is recommended in interpreting analyses concluding extreme effects of gas accumulation.

1 INTRODUCTION

In a deep geologic repository for radioactive waste, hydrogen would be generated by the anoxic corrosion of metallic components and by the radiolysis of water (King, 2007). Of these two sources, the dominant source of hydrogen is expected to be the anaerobic corrosion of the steel or copper waste container (with steel insert), according to a reaction such as that shown in Eq. (1-1).

$$3Fe + 4H_2O \rightarrow Fe_3O_4 + 4H_2 \quad (1\text{-}1)$$

Hydrogen production by this reaction will commence as soon as groundwater contacts the high-level waste container. Shoesmith (2007, 2008) states that dissolved hydrogen concentrations as high as 0.038 M at approximately 49 bar [706 psi] of hydrogen partial pressure are expected in "sealed" repositories.

The hydrogen would be generated in dissolved form. The ratio between the hydrogen fugacity in an existing gas phase and the dissolved hydrogen concentration in the liquid phase is governed by Henry's Law, with a Henry's constant of approximately 1282.1 atm/M at room temperature for the ratio of the partial pressure of hydrogen in the gas phase to dissolved hydrogen concentration in the groundwater (Young, 1981).

Additional complexities arise due to the potential formation of a hydrogen gas phase in the presence of buffer material. It is energetically more favorable for a gas phase to form in bulk water (i.e., when no porous medium is present) when dissolved gas species are supersaturated (Tanaka et al., 2003). If no gas phase is present (i.e., the buffer is completely water saturated), the dissolved hydrogen will spontaneously form gas bubbles once the dissolved hydrogen concentration reaches supersaturation. Supersaturation occurs when the sum of the fugacities from all dissolved gas species (e.g., H_2, O_2, N_2, and CO_2), and the water vapor pressure, exceeds the water liquid pressure. However, gas is not physically able to enter pore spaces unless the radius of curvature of the gas–water interface is small enough to fit into the pore. Thus, a gas phase is precluded from forming or migrating into a porous medium adjacent to a waste package unless the gas pressure exceeds the gas entry pressure of the porous medium (nominally the capillary pressure of the largest set of pores that could come into contact with the gas). This pressure accounts for the pressure increase across a curved interface (it increases as the pore size decreases). The air entry pressure for cracks, fractures, and gaps is much smaller than the air entry pressure for a typical buffer or host rock porous medium, so hydrogen bubbles will preferentially form in the largest openings (e.g., inside a waste package or at surface cracks) or at the edge of a porous medium (e.g., the contact between a metal surface and the porous medium), rather than in low permeability porous media.

Hydrogen generated at a metal surface will diffuse away from the source in the water phase, decreasing the dissolved hydrogen buildup at the source. If hydrogen generation is sufficiently rapid, the dissolved hydrogen concentration will exceed the saturation value; this could lead to formation of hydrogen bubbles at the interface. As long as there is sufficient space for bubble expansion, it is energetically favorable for hydrogen to diffuse towards and into the bubble. Conversely, if the gas bubble is restrained from expanding or moving (e.g., because of low permeability of the surrounding backfill or geologic medium), both the dissolved hydrogen concentration and the gas pressure in the bubble will increase. Eventually, either the gas pressure in the bubble may become large enough to rupture the restraining medium (i.e., form micro-cracks or transient dilational pathways) and escape, or additional bubbles will be created at other energetically favorable locations. Extensive information has been reported by Davy et

al. (2009), Lloret and Villar (2007), Xu et al. (2015), and Ye et al. (2014) on determining the total stress needed to rupture the buffer material and mechanical interactions between the buffer and generated gas that lead to buffer deformation. However, these complexities were not included in the model development.

Shoesmith (2007) argued that hydrogen fugacity could become as high as 50 bar [725.2 psi] in deep geologic repositories. High hydrogen fugacity is commonly cited as having the beneficial effect of decreasing spent nuclear fuel dissolution compared to oxidizing conditions. Important factors for determining the hydrogen concentration in groundwater and for evaluating the effects of hydrogen on spent fuel dissolution are the extent of possible hydrogen pressure buildup and the fugacity of hydrogen in deep geologic repository settings.

Bonin et al. (2000) provided a comprehensive review and analysis of various scenarios leading to the possible accumulation of hydrogen and pressure buildup in deep geologic repository systems. In particular, they noted that the repository designs presently considered in many countries tend to inhibit migration of chemical species originating within the repository by including long-lived watertight waste containers and low permeability engineered barriers. If the repository environment becomes saturated with water, the hydrostatic pressure—and therefore the maximal hydrogen pressure—could be approximately proportional to the depth of the repository. Thus, according to Bonin et al. (2000), the design features that limit ingress of water and migration of radionuclides also prevent hydrogen migration and may cause the pressure to build up in the near-field.

Xu et al. (2008) developed a coupled model to study the effect of hydrogen generation rate and its transport through the buffer medium in a nuclear waste repository. Xu et al. (2008) used a two-phase model to study H_2 gas generation, pressure buildup, and saturation distribution. The authors reported that for a hydrogen generation rate of approximately 2.0×10^{-12} mole/m^2/s, the hydrogen partial pressure could reach up to 81 bar after 5,000 years. In addition, when iron has completely corroded away, hydrogen generation will cease and hydrogen partial pressure will tend towards the background level equal to the hydrostatic pressure. The authors also reported that for a high corrosion rate of 2.0×10^{-11} mole/m^2/s, the gas pressure will increase to a peak pressure of 100 bar after 1,000 years, followed by gradual decrease. Iron disappears after about 23,000 years, which is much shorter than for the lower-rate base case, and the pressure recovers to the background pressure after 35,000 years.

Ortiz et al. (2002) studied gas generation and migration in a water-saturated clay medium, reporting that diffusive gas transport may be too slow compared to the gas generation rate. As a result, the gas pressure will build up around the gas generation source. The excess gas could cause fissures in the host rock in a direction perpendicular to the direction of the least effective stress. Thus, the excess gas will most probably migrate through a cyclic opening and closure of discrete preferential pathways in burst events, regulated by the gas pressure level at the onset of the pathways aperture.

Studying hydrogen generation, accumulation, and migration through buffer is complex and requires detailed coupled modeling of various processes, such as gas generation coupled with its diffusion through the buffer porewater, chemical interaction between the gas and the buffer medium, and feedback of local water activities on rates of hydrogen generation. This report focuses on developing a simplified model to estimate the gas accumulation in the buffer porewater under idealized conditions. The work by Bonin et al. (2000) is closely followed in developing the model. Chapter 2 provides a summary of carbon steel and copper corrosion

rates used for the model; Chapter 3 presents the model for hydrogen generation, accumulation, and migration; and Chapter 4 summarizes this work.

2 HYDROGEN GENERATION RATES

Hydrogen generation rates for carbon steel and copper were compiled from the literature and from the Center for Nuclear Waste Regulatory Analyses (CNWRA®) experimental data collected under reducing conditions. These data were used in modeling hydrogen accumulation and migration.

2.1 Carbon Steel

In a reducing repository, H_2 is produced by the cathodic reduction of H_2O or H^+. Corrosion of carbon steel proceeds via the reaction in Eq. (2-1), producing H_2:

$$Fe + 2H_2O \Leftrightarrow Fe(OH)_2 + H_2 \quad (2\text{-}1)$$

$Fe(OH)_2$ may convert to magnetite via the reaction in Eq. (2-2), also producing H_2:

$$3Fe(OH)_2 \Leftrightarrow Fe_3O_4 + 2H_2O + H_2 \quad (2\text{-}2)$$

Based on published studies, the stable anaerobic corrosion product of carbon steel is Fe_3O_4 rather than $Fe(OH)_2$. Therefore, the overall reaction for the anaerobic corrosion of carbon steel is written as in the reaction in Eq. (2-3).

$$3Fe + 4H_2O \Leftrightarrow Fe_3O_4 + 4H_2 \quad (2\text{-}3)$$

Based on the reaction in Eq. (2-3), 1.33 moles of H_2 are produced for each mole of Fe corroded. However, if both Fe_3O_4 and $Fe(OH)_2$ exist, the hydrogen produced for each mole of Fe is expected to lie between 1 and 1.33.

In the presence of compacted bentonite, it is reported that carbon steel corrodes with the formation of a carbonate corrosion product (Papillon et al., 2003; King, 2007, 2008) through the reaction in Eq. (2-4):

$$Fe + CO_3^{2-} + 2H_2O \Leftrightarrow FeCO_3 + H_2 + 2OH^- \quad (2\text{-}4)$$

Per the reaction in Eq. (2-4), 1 mole of H_2 is produced for each mole of Fe corroded.

Based on literature data, Jung et al. (2011) estimated corrosion rates for carbon steel in anoxic environments to be in the range of 0.1 to 10 μm/year [0.004 to 0.39 mils/yr]. King (2013) reported that the corrosion rates ranged between 0–18 μm/year at temperatures below 100 °C [212 °F]. In anoxic $Ca(OH)_2$ solution simulating concrete porewater, He et al. (2015) measured carbon steel corrosion rates of 0.1–3 μm/yr [0.004–0.1 mils/yr] at 30, 50, and 80 °C [86, 122, and 176 °F]. Therefore, 0.1 to 20 μm/yr is a reasonable range for corrosion rates in reducing conditions. The corrosion rate is converted to the molar production rate of hydrogen per unit surface according to Eq. (2-5):

$$j = f\frac{\rho_m V_c}{M_m} \quad (2\text{-}5)$$

where

j — hydrogen production rate (mole/m^2/sec)
ρ_m — density of the metal (g/m^3)
V_c — corrosion rate (m/sec)
M_m — molar mass of metal (g/mole)
f — moles of hydrogen produced per mole of iron

Carbon steel density is approximately 7.86 g/cm^3 and molar mass is 56 g. In addition, f is 1.33 as per Eq. (2-3). The calculated molar production rate of hydrogen ranges between 6×10^{-10} and 1.2×10^{-7} mole/m^2/sec. The corrosion and molar production rate data for carbon steel are summarized in Table 2-1.

2.2 Copper

In a reducing repository where O_2 is depleted, water could react with Cu through the reaction in Eq. (2-6):

$$2Cu + 2H_2O \Leftrightarrow 2CuOH + H_2 \quad (2\text{-}6)$$

According to the Pourbaix diagram, copper is thermodynamically stable in O_2-free environments. Therefore, copper corrosion is expected to be negligible in pure water. However, the repository groundwater is expected to contain ionic species that could promote copper corrosion. Groundwater transported from the far field could contain HS^-, Cl^-, SO_4^{2-}, and HCO_3^- in solution. According to the Pourbaix diagram, HS^- enhances copper reaction with anoxic water forming a Cu_2S film through the reaction in Eq. (2-7)

$$2Cu + HS^- + H_2O \Leftrightarrow Cu_2S + H_2 + OH^- \quad (2\text{-}7)$$

Based on the reactions in Eqs. (2-6) and (2-7), 0.5 moles of H_2 are produced for each mole of Cu corroded.

The depth of the corrosion front due to the reaction of copper with HS^- depends on the amount and transport of HS^- from the far field and on the Cu_2S film properties, including Cl^- effects.

Table 2-1. Corrosion and H_2 generation from carbon steel and copper waste container

Waste Container Material	Corrosion Reaction	Corrosion Rate in Reducing Environment, μm/yr	H_2 Generation Rate, moles/m^2/sec Waste Container Surface
Carbon steel	$3Fe + 4H_2O \Leftrightarrow Fe_3O_4 + 4H_2$ $Fe + CO_3^{2-} + 2H_2O \Leftrightarrow FeCO_3 + H_2 + 2OH^-$	0.1–20	6×10^{-10}–1.2×10^{-7}
Copper	$2Cu + 2H_2O \Leftrightarrow 2CuOH + H_2$ $2Cu + HS^- + H_2O \Leftrightarrow Cu_2S + H_2 + OH^-$	0.001–1 μm/yr	2.2×10^{-12}–2.2×10^{-9}

Taniguchi and Kawasaki (2008) measured copper corrosion rates in anoxic synthetic seawater with the addition of Na_2S using the weight loss method. The corrosion rate increased from less than 0.6, to 2–4, to 10–15 μm/yr [0.0234, to 0.078–0.156, to 0.39–0.585 mils/yr] as sulfide concentration increased stepwise from 0.001, to 0.005, to 0.1 M. In the absence of sulfide, the average corrosion rate was estimated to be 0.088 μm/yr [0.0034 mils/yr] over a test period of nearly 800 days. He et al. (2015) measured corrosion rates of copper exposed to simulated granitic groundwater, obtaining values of several tenths of a micrometer per year [several thousandths of mils per year] measured by electrochemical and weight loss methods. H_2 also was generated from the corrosion process reported in He et al. (2015). Based on examination of information in the literature, Jung et al. (2011) estimated copper corrosion rates in anoxic environments to be 4×10^{-3} to 2×10^{-2} μm/yr [2×10^{-4} to 8×10^{-4} mils/yr]. Considering the enhancement of copper corrosion by HS^-, copper corrosion rates in an anoxic environment are estimated to be in the range 0.001–1 μm/yr. Using Eq. (2-5) with a copper density of 8.96 g/cm^3 [0.323 lb/in^3] and $f = 0.5$, the H_2 generation rate is calculated to be 2.2×10^{-12}–2.2×10^{-9} moles/m^2/sec at the waste container surface. This information is summarized in Table 2-1.

3 HYDROGEN ACCUMULATION AND MIGRATION

For computing hydrogen accumulation and migration in porewater, it is assumed that the waste package is surrounded by a layer of the buffer material that is saturated with water and remains saturated as time elapses. As hydrogen is generated by the corrosion reaction, it will initially dissolve in the porewater and then migrate by diffusion. When the dissolved hydrogen concentration reaches saturation, the hydrogen at the waste package and bentonite interface will build up because the additional dissolved hydrogen diffuses away from the production area slowly. As more hydrogen is generated, hydrogen bubbles may form around the waste package. This will lead to formation of a two-phase fluid. It should be noted that local accumulation of hydrogen will lower the water activity, which in turn would slow down the corrosion and hydrogen production. This feedback is ignored in this simplified analysis.

A schematic representation of the system considered for model development is presented in Figure 3-1. In a host rock saturated with granitic groundwater, deep below the surface, the waste package is surrounded by the buffer. In the model, the depth to the waste package from the ground surface is larger than the saturated zone water column height above the waste package.

The evolution of the hydrogen concentration can be described as follows. At the beginning of the production process, the concentration of dissolved hydrogen in the porewater is c = 0 and porewater pressure is equal to

$$P_h = \rho_w g h_0 \tag{3-1}$$

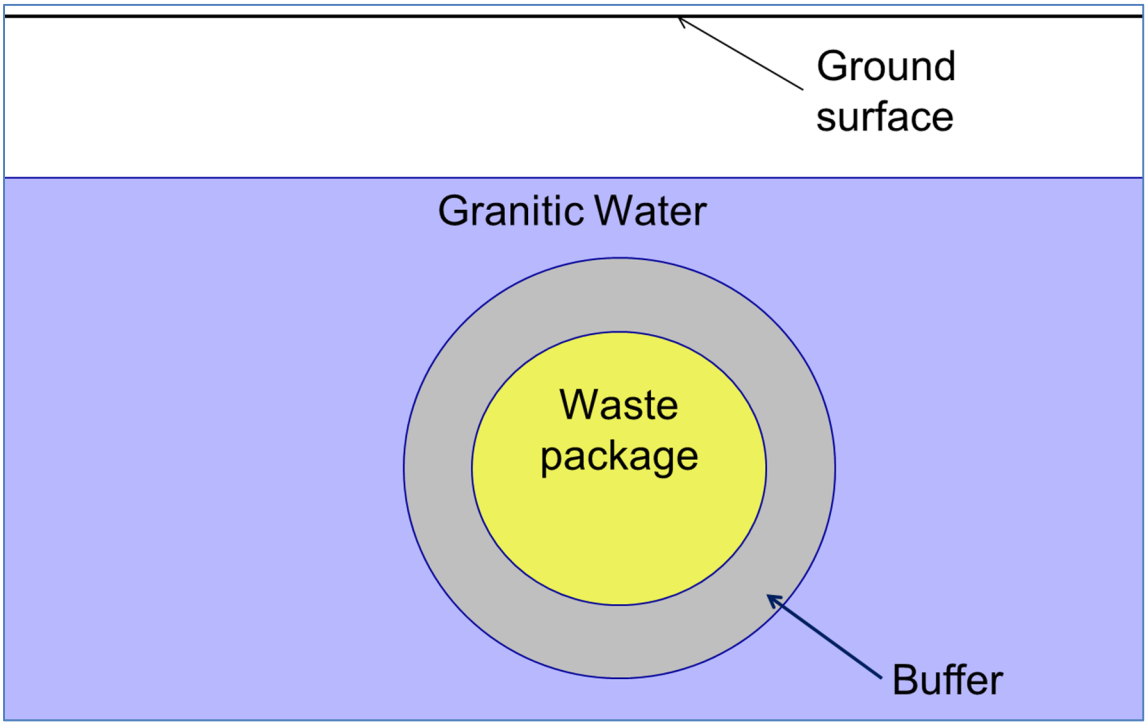

Figure 3-1. Schematic of the waste package and buffer system considered for the hydrogen accumulation and migration model

where

ρ_w — density of liquid water (g/m^3)
g — the gravity constant (m^2/sec)
h_0 — the repository depth with respect to the water table (m)

The dissolved hydrogen concentration increases with time, causing an increase of the pore pressure. This increase of pore pressure will be small if the buffer medium is very permeable or very compressible and large in the opposite case. Two conditions must be met for a gas phase to form: (i) the pressure in the bubble must equal the pore pressure plus the capillary pressure and (ii) the gas phase hydrogen must be in equilibrium with the dissolved hydrogen. The first condition can be expressed as

$$P_b = P_c + P_h \tag{3-2}$$

where

P_b — gas bubble pressure (Pa)
P_c — capillary pressure in the pores (Pa)

It is implicitly assumed that capillary pressure, which is a characteristic of the buffer medium and the two fluid phases, is well defined and is a singular value for the clay buffer. Whereas buffer materials contain a wide range of pore sizes, which would conceptually correlate with a range of capillary pressures, the pore size of interest is the set of interconnected large pores. The capillary pressure can be approximated by

$$P_c = \frac{2\sigma}{a} \tag{3-3}$$

where

σ — surface tension of the gas-water interface (N/m)
a — pore size of the buffer medium (m)

As per the second condition, dissolved hydrogen is assumed to be in instant equilibrium with the gas medium and is assumed to be in chemical equilibrium with the gas-phase hydrogen. This condition can be expressed by

$$P_b = \frac{c}{k_H} \tag{3-4}$$

where

c — dissolved hydrogen concentration (mol/L)
k_H — Henry's constant (mole/Pa/m^3)

Substitution of P_b in Eq. (3-2) yields:

$$P_h = \frac{c}{k_H} - P_c \tag{3-5}$$

where

c — dissolved hydrogen concentration
k_H — Henry's constant

The above expression defines a linear relation between pore pressure P_h and the dissolved hydrogen concentration at the metal and porewater interface. If the above equality is satisfied and the dissolved hydrogen concentration starts to exceed the saturation value, hydrogen will form as a bubble. However, the hydrogen also will migrate away from the waste package interface as a dissolved species through the porewater. The migration will occur due to diffusion and convection. Neglecting the convection, the hydrogen concentration in the $c(x,t)$ obeys the following equation

$$\frac{\partial c}{\partial t} = \frac{D_H}{\varepsilon}\nabla^2 c \tag{3-6}$$

where

D_H — diffusivity of the hydrogen in the porewater (m^2/sec)
ε — porosity of the buffer medium

In Eq. (3-6), it is implicitly assumed that there is no hydrogen source or sink in the buffer medium.

In the absence of a concentration gradient, the pore pressure would obey the usual piezometric equation in a permeable homogeneous compressible medium obeying Darcy's law according to the following equation

$$\frac{\partial P_h}{\partial t} = A\nabla^2 P_h \tag{3-7}$$

where A is the hydraulic diffusivity of the medium in units of m^2/sec. The effect of concentration variation on P_h can be accounted for by adding a time-dependent concentration variation term in accordance with the following equation:

$$\frac{\partial P_h}{\partial t} = A\nabla^2 P_h + \frac{1}{k}\frac{\partial c}{\partial t} \tag{3-8}$$

where $1/k$ is the rate of pressure increase due to concentration increase in a fixed volume of water. In the limiting case of a well-mixed system without concentration gradients, the value of k approaches k_H.

Eqs. (3-6) and (3-8) provide an approximate description of the concentration and pressure variation in the buffer medium. These equations are one-way coupled and can be solved to obtain an analytical solution. A simplified one-dimensional geometry of the system is assumed. The geometry is represented in a Cartesian system, with the interface of the waste package and buffer set to $x = 0$.

The boundary conditions for Eqs. (3-6) and (3-8) are as follows. At the waste package and buffer interface, the spatial gradient of the porewater pressure is related to the hydrogen generation rate according to the following condition (Bonin et al., 2000):

$$\left.\frac{\partial P_h}{\partial x}\right|_{x=0} = \frac{j}{K} g M_w \tag{3-9}$$

where

M_w	—	molar mass of water (g/mole)
j	—	hydrogen production rate (mole/m2/s)
K	—	saturated permeability of buffer medium in units (m/sec)

The above boundary condition describes the "sink term" associated with water consumption by the corrosion reaction. However, it is assumed that the metal and buffer interface is stationary. Similarly, the gradient of the hydrogen concentration at the waste package and buffer interface is related to the generation rate according to the following equation (Bonin et al., 2000):

$$\left.\frac{\partial c}{\partial x}\right|_{x=0} = -\frac{j}{D_H} \tag{3-10}$$

The initial conditions for the porewater pressure and dissolved hydrogen concentration are

$$P_h(x, t=0) = \rho_w g h_0 \tag{3-11}$$

and

$$c(x, t=0) = c_0 \tag{3-12}$$

It has been implicitly assumed that the gradient of the dependent variables (i.e., P_h and c) vanishes to zero at the far field. The analytical solutions of Eqs. (3-6) and (3-8), subjected to the boundary conditions in Eqs. (3-9) and (3-10) and the initial conditions in Eqs. (3-11) and (3-12), are

$$c(x=0, t) = 2j\sqrt{\frac{t}{D_H \varepsilon \pi}} + c_0 = 2j\sqrt{\frac{t}{D_H \varepsilon \pi}} + k_H \rho_w g h_0 \tag{3-13}$$

and

$$P_h(x=0, t) = \rho_w g h_0 + \frac{2}{\sqrt{\pi}} \frac{j}{\varepsilon k_H} \frac{1}{1 + \sqrt{D_H/\varepsilon A}} \sqrt{\frac{t}{A}} \tag{3-14}$$

The solution in Eq. (3-14) is adapted after Bonin et al. (2000). Clay and sand buffer media parameters for these calculations were developed from data in Bonin et al. (2000) and are provided in Table 3-1.

Table 3-1. Parameter values used to estimate the dissolved hydrogen concentration	
Parameter	**Value for a Clay-Based Buffer**
Porosity, ε	0.2
Capillary pressure, P_c (Pa)	1.3×10^5 to 10^7
Hydraulic diffusivity, A (m^2/sec)	3×10^{-9}
Hydrogen diffusion coefficient, D_H (m^2/sec)	10^{-11}
Saturated Permability, K (m/sec)	10^{-12}
Density, ρ_w (kg/m^3)	1,000 kg/m^3
Continuous depth of water column, h_0 (m)	5, 100, 300, and 500
Henry's constant, k_H (mole/Pa/m^3)	7.6×10^{-6}

Eq. (3-13) indicates that the hydrogen concentration increases with time without an upper bound. In reality, however, the solution and gas phases may separate, with the hydrogen gas phase satisfying the thermodynamic equilibrium of Eq. (3-5). Assuming that all of the hydrogen remains in solution throughout, the minimum time to reach saturation at the position $x = 0$ is obtained by substituting $c(x = 0, t)$ and $P_h(x = 0, t)$ into Eq. (3-5):

$$t_b = \frac{\pi}{4A}\left(\frac{P_c \varepsilon k_H}{j}\right)^2 \left[\frac{D_H}{\varepsilon} + \sqrt{\frac{D_H A}{\varepsilon}}\right]^2 \tag{3-15}$$

Eqs. (3-13) and (3-15) were programmed in MATLAB (Mathworks, 2008) to calculate hydrogen concentration profiles as a function of time. Calculated dissolved hydrogen concentrations at $x = 0$ (assuming no degassing) for clay buffer as a function of time are presented in Figures 3-2 and 3-3 for capillary pressure of 10^7 Pa.

If the capillary pressure is much lower than the hydrostatic pressures at the repository depths considered in this work, the saturated concentration of dissolved hydrogen is simply equal to the hydrostatic pressure multiplied by the Henry's constant. Therefore, hydrogen will accumulate in the gas phase and begin migrating into the buffer as soon as its partial pressure exceeds the hydrostatic pressure in a buffer medium where capillary pressure is lower than the hydrostatic pressure. The simulation results in Figures 3-2 and 3-3 are for a capillary pressure of 10^7 Pa.

As seen in Figure 3-2 for the carbon steel corrosion rate of 0.1 μm/year, the dissolved hydrogen concentration increases with time and reaches a maximum value in about 800 years. The

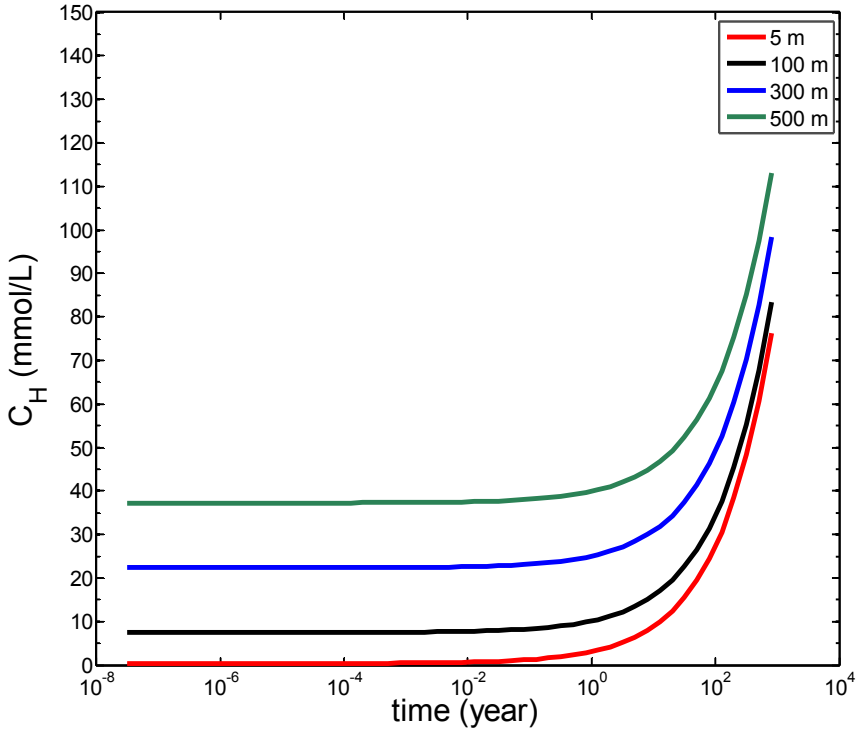

(a) Carbon Steel Corrosion Rate of 0.1 μm/year

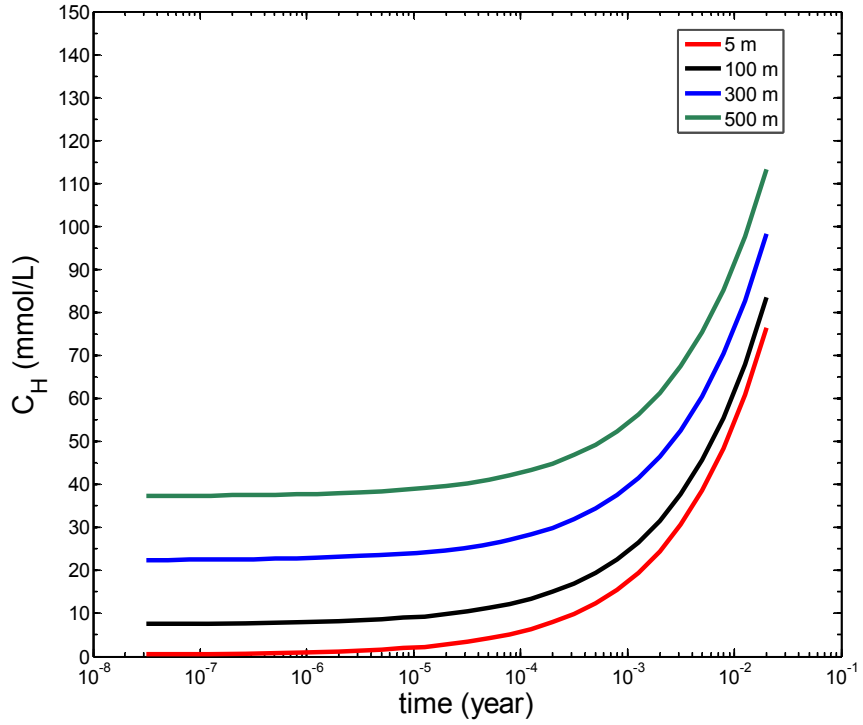

(b) Carbon Steel Corrosion Rate of 20 μm/year

Figure 3-2. Dissolved hydrogen concentration at the waste package and clay buffer interface for carbon steel corrosion rates of (a) 0.1 and (b) 20 μm/year for 5, 100, 300, and 500 m of continuous water column with respect to the water table

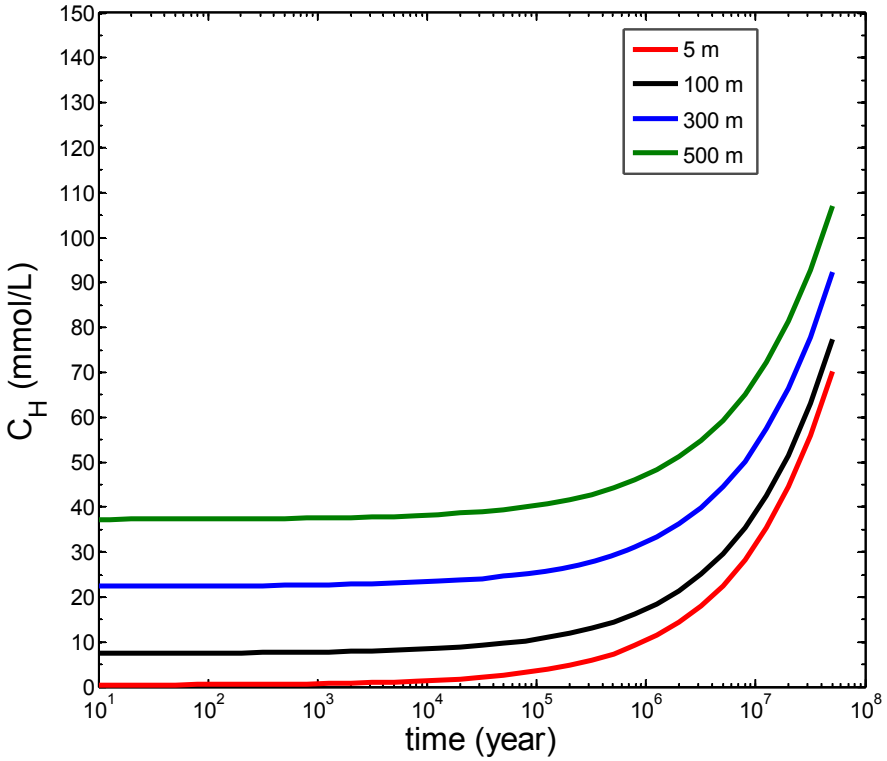

(a) Copper Corrosion Rate of 10^{-3} μm/year

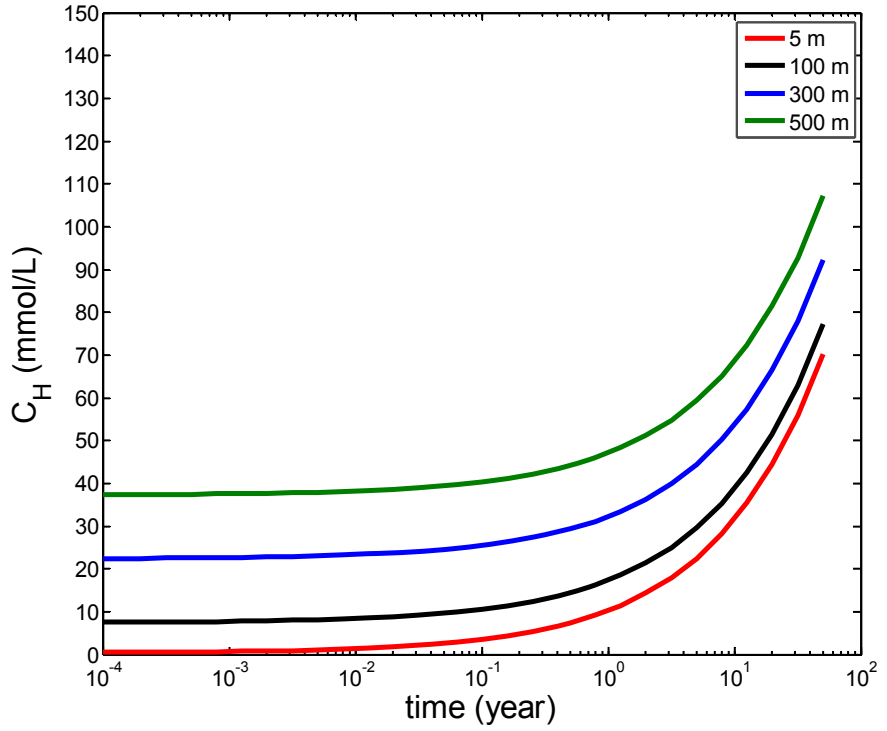

(b) Copper Corrosion Rate of 1 μm/year

Figure 3-3. Dissolved hydrogen concentration at the waste package and clay buffer interface for copper corrosion rates of (a) 10^{-3} and (b) 1 μm/year for 5, 100, 300, and 500 m of continuous water column with respect to the water table

endpoint of the curves in Figure 3-2 is the time to saturation as calculated from Eqs. (3-13) and (3-15). For the corrosion rate of 20 μm/year, the maximum dissolved hydrogen concentration is reached in approximately 10^{-2} years (note, however, that hydrogen degassing was ignored in the computation of this minimum time). The curves for dissolved hydrogen concentration at $x = 0$ versus time are the same shape for low and high carbon steel corrosion rates; only the times to reach the maximum concentration differ. This observation is consistent with Eq. (3-13), in which dissolved hydrogen concentration has a linear dependence on the corrosion rate.

As seen in Figure 3-3 for the copper corrosion rate of 10^{-3} μm/year, the dissolved hydrogen concentration increases with time and reaches a maximum value in about 50 million years. Similar to Figure 3-2, the endpoint of the curves in Figure 3-3 is the time to saturation as calculated from Eqs. (3-13) and (3-15). For the corrosion rate of 1 μm/year, the maximum dissolved hydrogen concentration is reached in approximately 50 years. As previously stated, these are minimal times, assuming no hydrogen degassing from the solution. As in the carbon steel case, the shapes of the dissolved hydrogen concentration versus time curves for low and high copper corrosion rates are the same.

Highlighting the effect of capillary pressure, simulation results for a capillary pressure of 1.3×10^5 Pa and a carbon steel corrosion rate of 20 μm/year are presented in Figure 3-4. As seen in the figure, the maximum dissolved hydrogen concentration only marginally changes with the respect to the initial concentration. On the other hand, as seen in Figure 3-2(b), the maximum dissolved hydrogen concentration increases by factor of 3 to 10 for the capillary pressure of 10^7 Pa. This clearly indicates that a buffer with higher capillary pressure will result in higher dissolved hydrogen concentration in the groundwater compared to a buffer with lower capillary pressures, assuming other conditions are the same.

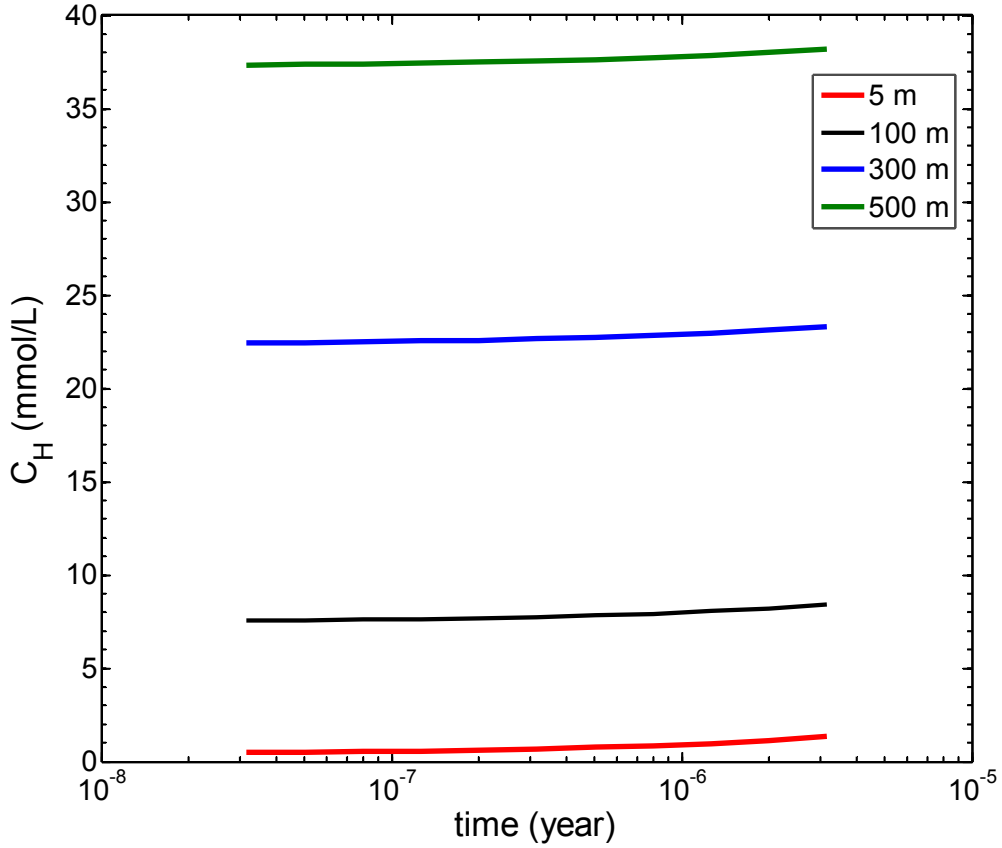

Figure 3-4. Dissolved hydrogen concentration at the waste package and clay buffer interface for carbon steel corrosion rates of 20 μm/year for 5, 100, 300, and 500 m of continuous water column with respect to the water table and capillary pressure of 1.3 × 10^5 Pa

4 SUMMARY AND DISCUSSION

A simplified model was developed to compute hydrogen concentration in buffer porewater contacting a waste package in a hypothetical repository. The model, developed following the work of Bonin et al. (2000), was used to compute the minimum time for the hydrogen concentration to saturate the solution, ignoring hydrogen degassing from the solution. The model was exercised to estimate the dissolved hydrogen concentration in porewater at the waste package-buffer material interface as a function of carbon steel and copper corrosion rates, depth with respect to the water table, and clay-based bentonite buffer parameters.

The results indicate that for low corrosion rates of carbon steel in the clay-based buffer, the hydrogen concentration in the porewater directly in contact with the waste package could saturate in approximately 800 years (minimal time ignoring degassing). The dissolved hydrogen concentration increases with time and, for a given time, with increasing depth with respect to the water table. The model results also indicate that for high corrosion rates of carbon steel in the clay-based buffer, the hydrogen concentration in the porewater directly in contact with the waste package may saturate the solution within a few days. For this case also, the dissolved hydrogen concentration increases with time and, for a given time, with increasing depth with respect to the water table. The overall shapes of the hydrogen concentration (at $x = 0$) versus time curves are the same for the two cases. The model results for copper are similar in behavior to the carbon steel results, but the magnitudes of the minimum saturation times differ significantly. For the low copper corrosion rate, the dissolved hydrogen concentration reaches the saturation value in approximately 50 million years or more. However, for the high corrosion rate of copper, the saturation level is reached in approximately 50 years.

The corrosion rate is an important parameter, along with buffer properties, in determining accumulation and migration of hydrogen. It should be noted that this simplified analysis neglected coupling and feedback effects. For example, local accumulation of hydrogen at the waste package-buffer interface would reduce the water activity, which in turn would decrease the rate of corrosion and hydrogen production. Local accumulation of hydrogen implies that hydrogen cannot easily disperse, which would be an indication of an impermeable system through which the decomposed water is not quickly replenished. Limiting the availability of water also slows down the rate of production of hydrogen. In other words, features such as impermeability, which seems to hypothetically enhance gas buildup effects in the system, also work against the availability of water, thus constraining the production of hydrogen. Most, if not all, analyses in the literature, including the analysis in this report, are designed to maximize some gas buildup effects and ignore couplings and competing effects that would counteract the gas buildup. In this project, it was identified that developing fully coupled models allowing full examination of the relevance of gas buildup is most challenging. Some processes are not characterized well enough to allow for detailed modeling. For example, spent fuel dissolution rates as a function of hydrogen gas concentration, metal corrosion rates as a function of water activity, and the slow water saturation process of buffer materials are not entirely well understood and characterized. Thus, uncertainties are abundant and prevent unequivocally establishing the relevance of gas buildup. Conclusions in the literature asserting detrimental gas buildup effects should be treated with caution, as those analyses are in general designed to maximize those effects. In this report, we explored the solution saturation time as a metric to examine a range of possibilities, and we found that the saturation time varies broadly as a function of corrosion rates, distance with respect to the water table, and buffer material properties.

5 REFERENCES

Bonin, B., M. Colin, and A. Dutfoy. "Pressure Building During the Early Stages of Gas Production in a Radioactive Waste Repository." *Journal of Nuclear Materials*. Vol. 281. pp. 1–14. 2000.

Davy, C.A., F. Skoczylas, P. Lebon, and T. Dubois. "Gas Migration Properties Through a Bentonite/Argillite Interface." *Applied Clay Science*. Vol. 42. pp. 639–648. 2009.

He, X., T. Ahn, and J. McMurry. "Literature Review and Experiments on Waste Package Corrosion—Copper and Carbon Steel." ML16014A269. Washington, DC: U.S. Nuclear Regulatory Commission. 2015.

Jung, H., T. Ahn, and X. He. "Representation of Copper and Carbon Steel Waste Package Degradation in a Generic Performance Assessment Model." Proceedings of 2011 International Radioactive Waste Management Conference (IHLRWMC), Albuquerque, New Mexico, April 10–14, 2011. Paper No. 3353. 2011.

King, F. "Consequences of the General Corrosion of Carbon Steel Used Fuel Containers for Gas Generation in a DGR." NWMO TR-2013-16. Toronto, Canada: Nuclear Waste Management Organization (NWMO). 2013.

King, F. "Corrosion of Carbon Steel under Anaerobic Conditions in a Repository for SF and HLW in Opalinus Clay." Nagra Technical Report NTB 08-12. Nagra, Wettingen, Switzerland. 2008.

King, F. "Overview of a Carbon Steel Container Corrosion Model for a Deep Geological Repository in Sedimentary Rock." TR–2007–01. Toronto, Canada: Nuclear Waste Management Organization (NWMO). 2007.

Lloret, A., and M.V. Villar. "Advances on the Knowledge of the Thermo-Hydro-Mechanical Behavior of Heavily Compacted FEBEX Bentonite." *Physics and Chemistry of the Earth*. Vol. 32. pp. 701–715. 2007.

Mathworks. "MATLAB User's Guide." Natick, Massachusetts: The MathWorks, Inc. 2008.

Ortiz, L., G. Volckaert, and D. Mallants. "Gas Generation and Migration in Boom Clay. A Potential Host Rock Formation for Nuclear Waste storage." *Engineering Geology*. Vol. 64. pp. 287–296. 2002.

Papillon, F., M. Jullien, and C. Bataillon. "Carbon Steel Behavior in Compacted Clay: Two Long Term Tests for Corrosion Prediction." In: Prediction of Long Term Corrosion Behavior in Nuclear Waste Systems. European Federation of Corrosion Publication No. 36 (Institute of Materials, Minerals and Mining, London). Chapter 29. pp. 439–454. 2003.

Shoesmith, D.W. "The Role of Dissolved Hydrogen on the Corrosion/Dissolution of Spent Nuclear Fuel." NWMO TR-2008-19. Toronto, Ontario, Canada: Nuclear Waste Management Organization. 2008.

Shoesmith, D.W. "Used Fuel and Uranium Dioxide Dissolution Studies—A Review." NWMO TR-2007-03. Toronto, Ontario, Canada: Nuclear Waste Management Organization. 2007.

Taniguchi, N. and M. Kawasaki. "Influence of Sulfide Concentration on the Corrosion Behavior of Pure Copper in Synthetic Water." *Journal of Nuclear Materials*. Vol. 379. pp. 154–161. 2008.

Tanaka, Y., S. Uchinashi, Y. Saihara, K. Kikuchi, T. Okaya, and Z. Ogumi. "Dissolution of Hydrogen and the Ratio of the Dissolved Hydrogen Content to the Produced Hydrogen in Electrolyzed Water Using SPE Water Electrolyzer." *Electrochimica Acta*. Vol. 48. pp. 4,013–4,019. 2003.

Xu, L., W.M. Ye, B. Ye, B. Chen, Y.G. Chen, and Y.J. Cui. "Investigation on Gas Migration in Saturated Materials with Low Permeability." *Engineering Geology*. Vol. 197. pp. 94–102. 2015.

Xu,T., R. Senger, and S. Finsterle. "Corrosion-Induced Gas Generation in a Nuclear Waste Repository: Reactive Geochemistry and Multiphase Flow Effects." *Applied Geochemistry*. Vol. 23. pp. 3,423–3,433. 2008.

Young, C. L., ed. "IUPAC Solubility Data Series." Vol. 5/6, Hydrogen and Deuterium. Pergamon Press. Oxford, England. 1981.

Ye, W.M., L. Xu, B. Chen, Y.G. Chen, B. Ye, and Y.J. Cui. "An Approach Based on Two-Phase Flow Phenomenon for Modeling Gas Migration in Saturated Compacted Bentonite." *Engineering Geology*. Vol. 169. pp. 124–132. 2014.